Capacity and Energy Efficiency of TeraHertz Surface Wave Interconnects

Qing, Jie; Navarro-Cia, Miguel

[Link to publication on Research at Birmingham portal](#)

RESEARCH ARTICLE

ADVANCED
PHOTONICS
RESEARCH
Open Access

www.adpr-journal.com

Capacity and Energy Efficiency of TeraHertz Surface Wave Interconnects

Jie Qing and Miguel Navarro-Cía*

The potential of geometrically induced terahertz surface wave technology for communications can only be realized if communication links based on them are studied and benchmarked. The frequency-dependent transmission characteristics of interconnects based on three different archetypal textured surfaces (namely, gratings, dominos, nails) are analyzed numerically and the impact of the geometry and realistic surface roughness on the maximum capacity and energy efficiency is quantified. Unlike conventional hollow waveguides, the analysis shows that the capacity of uncoated corrugated surfaces is limited by loss and not dispersion. This work provides the guidelines for the design of terahertz surface wave interconnects.

1. Introduction

The volume of data that needs to be transferred is continuously increasing with the arrival of new applications and the growth of high-definition video usage. Consequently, there is an urgent need to achieve a transfer rate of terabits per second (Tbps) for both wireless and chip-to-chip connections. However, reaching such a high bit rate is currently not possible unless we shift the carrier frequency from current microwaves to TeraHertz (THz) frequencies.[1] Unfortunately, in the context of chip-to-chip communications, the development of interlinks at these high frequencies is still pending.[2] One potential solution for establishing such interlinks involves utilizing highly confined surface waves[3] instead of volumetric waveguides that are ill-advised for integration.

J. Qing
Terahertz Science and Technology Research Center
University of Electronic Science and Technology
Chengdu 610056, China

J. Qing, M. Navarro-Cía
School of Physics and Astronomy
University of Birmingham
Birmingham B15 2TT, UK
E-mail: M.NavarroCia@bham.ac.uk

M. Navarro-Cía
Department of Electronic, Electrical and System Engineering
University of Birmingham
Birmingham B15 2TT, UK

The ORCID identification number(s) for the author(s) of this article can be found under https://doi.org/10.1002/adpr.202300250.

Surface waves have been extensively studied in both microwave engineering[4,5] and the fields of physics/optics,[6] often using different terms to describe the same complex wave phenomenon[4,7] (e.g., geometrically induced surface wave, spoof surface plasmon, and designer surface plasmon when discussing surface wave on textured metal surfaces). The most commonly used method to realize highly confined surface waves at THz frequencies is through the use of various textured metal surfaces.[8–10] While the attenuation and dispersion characteristics of these geometrically induced THz surface waves are well understood,[4,5,7–13] their application in the context of communications has not been systematically explored yet. Without a quantitative system analysis, any discussion about future THz surface wave links is unfounded.

To address this knowledge gap, we present a system analysis of geometrically induced THz surface wave links in terms of their capacity (measured in bps) and energy efficiency (measured in J bit^{-1}).[14] For this analysis, we benchmark three of the most popular textured surfaces supporting geometrically induced THz surface waves, namely grating, domino, and bed of nails. These three-dimensional (3D) platforms are chosen here instead of the more integrable planar counterparts (i.e., spoof surface plasmons polariton waveguides) for two reasons: 1) the planar versions require substrates and therefore pose dielectric losses that are of significant concern at THz frequencies and[15] 2) 3D platforms may be more suitable for scenarios with large metal parts such as airplane and drone fuselages, desktop chassis, etc. that can be textured to realize the interconnect. For the numerical study to be of practical usability, we consider the impact of realistic surface roughness to provide a realistic best-case analysis. Although the work is numerical and no measurements are reported here, the mode dispersion and attenuation calculation methodology that forms the ancillary knowledge for the system analysis have been recently validated.[16]

2. Physical Characteristics of the Link

Attenuation and dispersion are the ancillary propagation characteristics of any transmission line from which to build up channel propagation models and system analysis. Hence, we review these characteristics for three representative textured aluminum surfaces (1D grating and 2D array of dominos and nails, see **Figure 1**) before reporting the secondary information capacity and energy efficiency. We consider both ideal perfect textured surfaces and
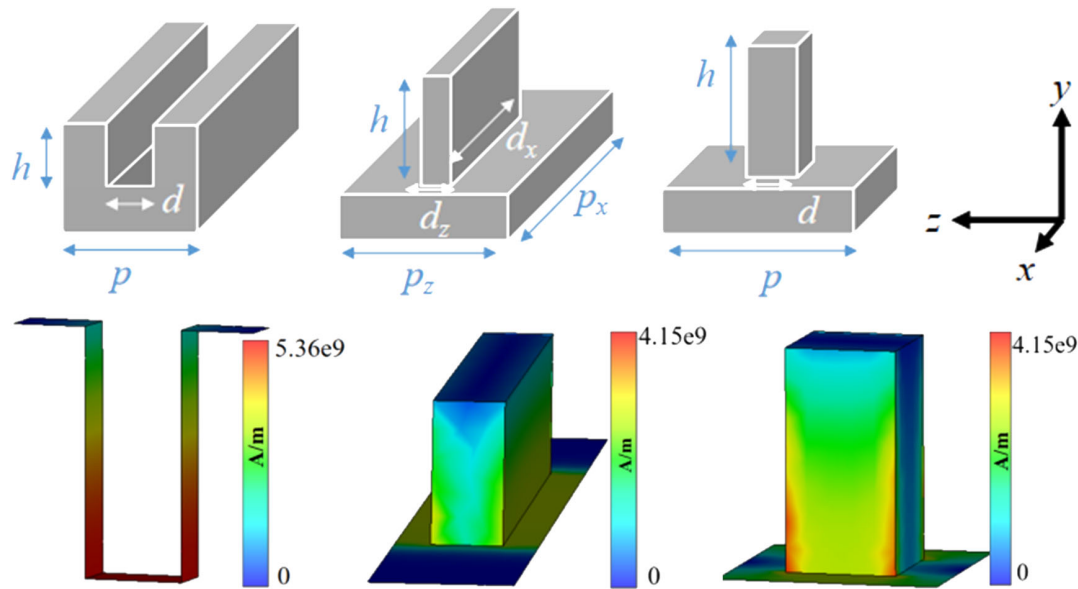
Figure 1. Unit cell diagrams of the textured platforms and surface currents at the surface wave frequency. The geometrical parameters of the structures h, d, p, d_x, d_z, p_x, p_z are visually defined in the top row.

textured surfaces with realistic surface roughness measured from laser machined prototypes.[16] The roughness is modeled as a Gaussian height distribution function matching the measured root-mean-square surface roughness (5 μm, unless otherwise stated) and a Gaussian autocovariance function with correlation length of 0.01 mm.

2.1. Dispersion Characteristic

The dimensions, presented in **Table 1**, are designed to support a surface wave in the range of 0.4–0.6 THz, see **Figure 2**a, and consider current fabrication limitations of laser machining.[16] This frequency range is chosen to match one of the proposed bands for future THz communication systems.[17] The dispersion characteristics of all structures displayed in Figure 2 are computed using the Eigenmode Solver of CST Microwave Studio, whose accuracy for surface wave dispersion calculation has been tested against measurements in the past.[16]

The dispersion diagram shown in Figure 2a along with the corresponding group delay

$$\tau = \frac{\partial \beta}{\partial \omega} \tag{1}$$

shown in Figure 2b demonstrates that surface roughness has a large impact on the grating dispersion causing the surface wave frequency (i.e., the asymptotic frequency) to redshift ≈27 GHz

Table 1. Designed unit cell dimensions of each structure.

	d or d_x/d_z [mm]	p or p_x/p_z [mm]	h [mm]
Grating	0.04	0.1	0.1
Dominos	0.5/0.05	1/0.1	0.1
Nails	0.05	0.1	0.1

from 0.597 to 0.570 THz. Meanwhile, the impact of the roughness is minimal on the 2D array of dominos and nails, with a blueshift of 11 GHz (from 0.583 to 0.594 THz) and 5 GHz (from 0.590 to 0.595 THz), respectively. These different impacts will be translated to the capacity of the links as shown later.

2.2. Attenuation Characteristic

The path loss in dB cm^{-1} of the three geometrically induced THz surface waves shown in Figure 1 is computed through a cutback-like method[18] whereby

$$\alpha = -\frac{4.343 \cdot [\ln(|E(\omega)_{d2}|^2/|E(\omega)_{d1}|^2)]}{\Delta d} \tag{2}$$

where $E(\omega)_d$ is the E-field amplitude at position d along the structure and Δd is the difference between two positions $d1$ and $d2$. This path loss is composed of Ohmic, α_{ohmic}, scattering (due to surface roughness), α_{scatt}, and propagation divergence loss,[16] that we model here as an equivalent exponential attenuation, $\alpha_{spreading}$, for simplicity. All these different loss mechanisms are disentangled through a set of time domain simulations with aluminum (3.56×10^7 S m^{-1}) as metal model: Ohmic and scattering losses are calculated from 2D simulations that assume the structure infinitely periodic in the x-direction, whereas the propagation divergence loss is computed from 3D simulations without surface roughness. To map accurately the rough surface within our computational resources, a fine hexahedral mesh of 2 μm × 2 μm × 2 μm was used. Time-domain CST MWS stopped when the remaining energy in the simulation was 80 dB below the peak value.

Figure 3 presents the path loss of the geometrically induced THz surface wave supported by each of the three geometries. This path loss level is 3 orders of magnitude higher than those
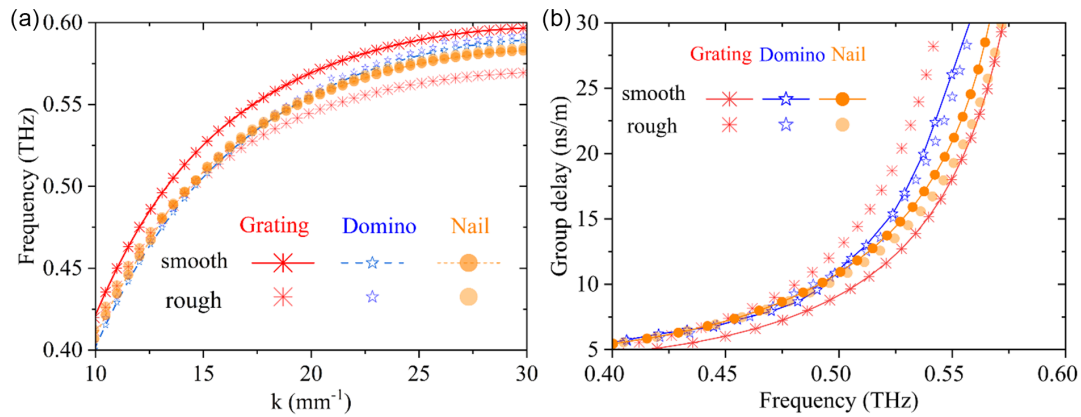
Figure 2. a) Dispersion curves corresponding to rough and smooth surfaces. b) Group delay.
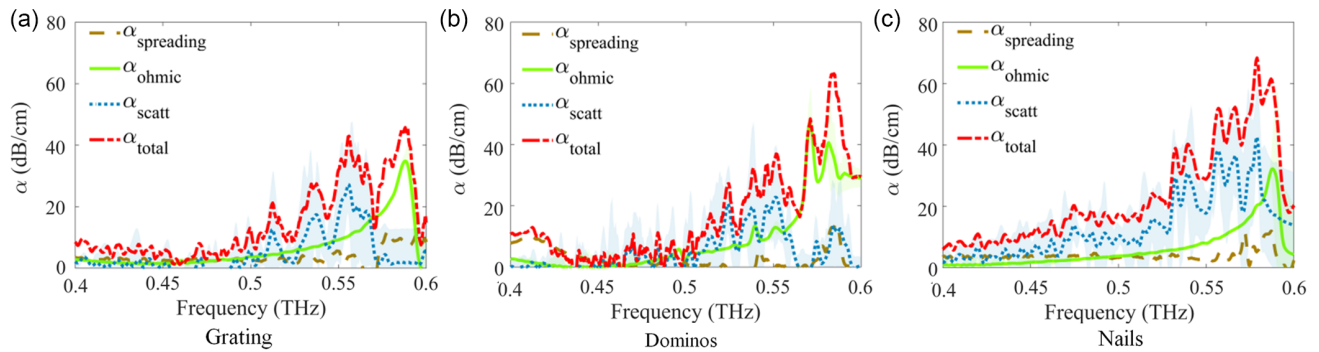
Figure 3. $\alpha_{spreading}$, α_{ohmic}, α_{scatt}, and α_{total} for the a) grating, b) array of dominos, and c) array of nails. Modeled surface roughness (root mean square) was 5 μm as per measurements of laser-machined prototypes. The blue dotted lines correspond to the average value of α_{scatt} over the six combinations from four software-defined probes equispaced 5 mm and the corresponding shaded regions illustrate the standard deviation of the results.

reported for millimeter-wave dielectric waveguides,[14] which should restrict the use of geometrically induced THz surface waves to short distance communications as those on on-chip applications. From the surface currents in Figure 1b, one should expect the nail to display the lowest α_{ohmic} approaching surface wave frequency; this is confirmed in Figure 3. However, the total path loss of the nails is the highest as a result of the other attenuation contributions. The α_{ohmic} and α_{scatt} increase with frequency because of the increasing interaction time (lower group velocity of the surface wave as shown in Figure 2b) and confinement, and $\alpha_{spreading}$ is only noticeable for nails since the nail is the only one with an isotropic dispersion diagram on the xz plane.

3. Capacity and Energy Efficiency

3.1. Capacity Limited by Dispersion

In digital data transmission, the maximum achievable data rate for a given distance and operating frequency can be determined as[19]

$$C = [(\tau(\omega_0 + \Delta\omega) - \tau(\omega_0 - \Delta\omega)) \cdot L]^{-1} \tag{3}$$

where τ is the group delay per unit length, ω_0 is the carrier frequency, and the L is the length of the interconnect. The proposed

bandwidth for future services in the frequency band 275–450 GHz ranges from 2 GHz to 65 GHz[20]; here we take the value of $\Delta\omega$ as 30 GHz without loss of generality. **Figure 4** shows the maximum applicable data rate versus link length when the carrier frequency is 0.45, 0.5, and 0.55 THz for smooth and rough textured surfaces corresponding to different colors and line labels.

It shows that different textured surfaces exhibit different transfer performances at the same operating frequency, while having similarity due to the uniformity of the dispersion relationship. That the data rate decreases as frequency increases seems counterintuitive, especially when comparing against millimeter-wave dielectric waveguide links.[14] However, this is the natural consequence of the higher dispersion of surface waves as the frequency approaches the asymptotic surface wave frequency. As anticipated earlier, surface roughness has a nontrivial impact on the capacity. For the dominos and nails, surface roughness tends to deteriorate the capacity of the link. For grating surface waves, however, surface roughness leads to a counterintuitive increase of capacity. Tbps is only achievable for distances <1 mm, which reinforces the earlier conclusion from the path loss results that surface wave links will be restricted to short distances such those on interconnects.
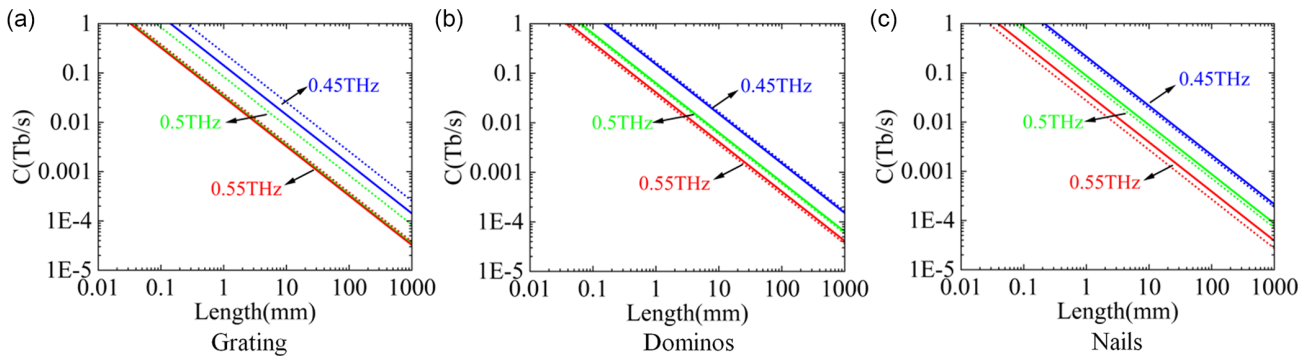
Figure 4. The maximum applicable data rate versus the length for the a) grating, b) array of nails, and c) array of holes operating at different center frequencies (0.45 THz -blue-, 0.5 THz -green-, and 0.55 THz -red-) for perfect (solid line) and rough textured surface (dotted line).

3.2. Energy Efficiency

The energy efficiency of the link is influenced by the geometry of the link, the operating frequency, the required capacity, and the attenuation of the link, and these parameters are intertwined. Quantifying the energy efficiency of the link provides a single metric for the design of the link. In the transmitter side, an output power of[14]

$$P_{out,TX} = -174\,\text{dBm} + 10\log \text{BW} + \text{SNR} + \text{NF}_{RX} + \alpha \cdot L \qquad (4)$$

is required to address the link budget. $\text{BW} = 2\Delta\omega$, SNR is the required signal-to-noise ratio at the receiver, NF_{RX} is the receiver noise figure. Energy efficiency is thus calculated by dividing the total power consumption to the maximum achievable data rate.[21]

$$\text{Energy efficiency} = \frac{P_{out,TX}}{C_{max,\,binary\,signal}} \qquad (5)$$

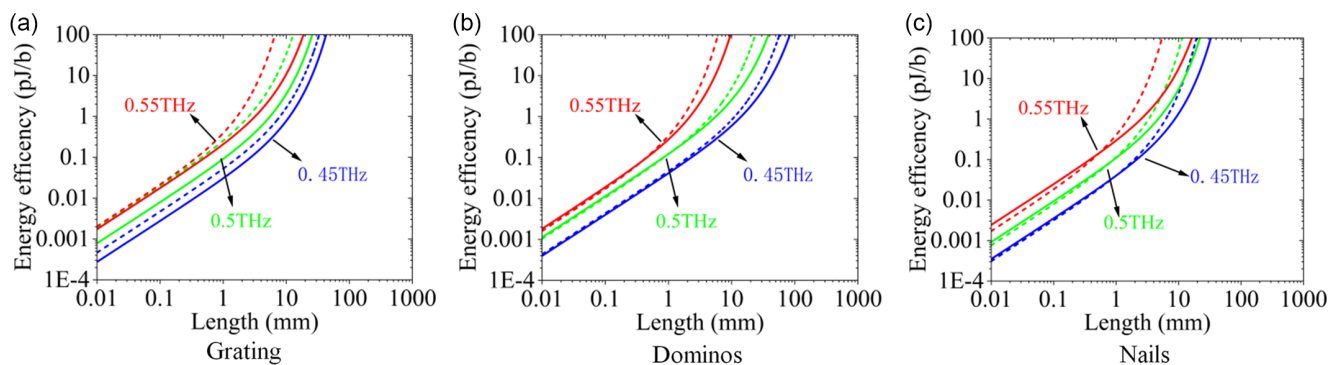**Figure 5** shows the corresponding energy efficiency in terms of pJ bit^{-1} assuming binary phase shift (BPSK) modulation, a bit error rate requirement of 10^{-12}, and $\text{NF}_{RX} = 10$ dB. As expected by inspecting Equation (4) and (5), the increasing path loss with frequency results into poorer energy efficiency for higher center frequencies. This is consistent with dielectric waveguides in which energy efficiency worsens with higher center frequencies;

however, in those waveguides, this is accompanied with higher data rates. This indicates that terahertz surface wave links are limited by attenuation rather than dispersion as it is the case for dielectric waveguides. The impact of roughness on energy efficiency is again nontrivial; in general, roughness results in poorer energy efficiency, but the opposite happens in dominos and nails for $L < 1$ mm.

We extend the analysis considering other values of surface roughness and conductivity for a link length of 1 mm. The top row in **Figure 6** depicts the energy efficiency for several levels of surface roughness ranging from a surface roughness free platform to one with 10 μm when the conductivity is 3.56×10^7 S m^{-1}; for the worst-case scenario that corresponds to the grating, the energy efficiency worsens by a factor of over 3. Meanwhile, the energy efficiency for reducing values of conductivity shown in the bottom row of Figure 6 demonstrates that lowering the conductivity by a factor of ≈ 7 yields an energy efficiency reduction by a factor ≈ 2 at worst.

4. Comparison against the Literature

There is an increasing interest in the topic of on-chip communication links at millimeter-waves and THz. To capture this work in this context, we tabulate in **Table 2** the performance of reported studies along with that for the here studied geometrically induced terahertz surface wave interconnects of 10 mm.

Figure 5. The corresponding energy efficiency (pJ bit^{-1}) for the a) grating, b) array of dominos, and c) array of nails operating at different center frequencies (0.45 THz -blue-, 0.5 THz -green-, and 0.55 THz -red-) for perfect (solid line) and rough textured surface (dotted line).

2300250 (4 of 6)
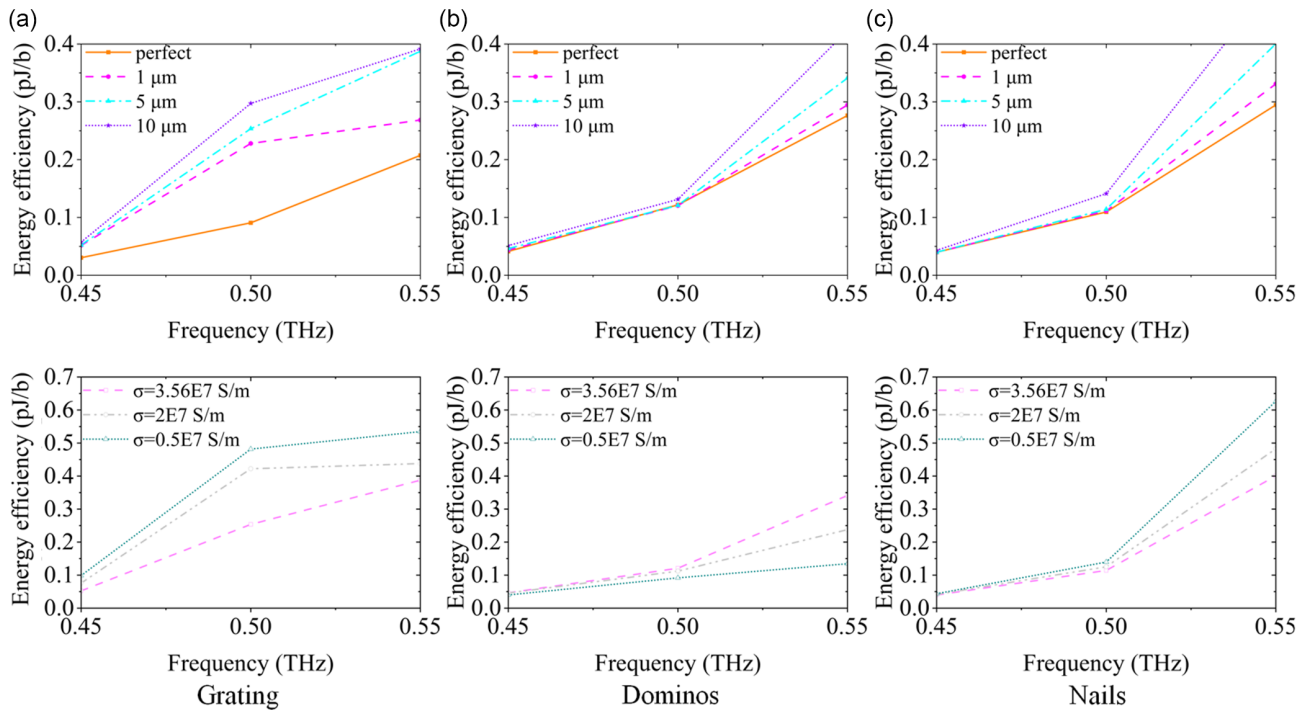
Figure 6. Energy efficiency (pJ bit^{-1}) for varying values of surface roughness with a conductivity of 3.56×10^7 S m^{-1} (top) and varying values of metal conductivity with a surface roughness of 5 µm (bottom) for a 1 mm-long link based on the a) grating, b) array of dominos, and c) array of nails.

Table 2. Key performance indicators of reported on-chip communication links.

Frequency	Modulation	Waveguide type	Distance	Capacity [Gb s^{-1}]	Energy efficiency [pJ b^{-1}]	References
500 GHz	BPSK	Surface:	–	–	–	Here
		Grating	10 mm	8	35	
		Dominos	10 mm	6	5	
		Nails	10 mm	7	60	
87 GHz	Multilevel ASK	Rectangular dielectric	0.6 m	9	5.6	[22]
			9 m	2.5	20	
140 GHz	ASK (non-coherent)	Planar spoof plasmon	20 mm	25	0.32	[23]
120 GHz	CPFSK	Hollow dielectric	1 m	12.7	4.8	[24]
			4 m	7.4	7.2	
			7 m	2.5	28.7	
165 GHz	OOK	Microstrip	8.1 mm	9	7.7	[25]
165 GHz	OOK	Dielectric	46.2 mm	10	0.32	[26]
140 GHz	CPFSK	Foam-clad dielectric	2 m	10	–	[27]
			4 m	7		
1 THz		Planar spoof plasmon	10 mm	300	–	[28]
150 GHz	PAM-4	Dielectric (plastic PCB)	50 mm	30	2.01	[29]
58 GHz	QAM-16	Hollow dielectric	1 m	34	–	[30]
83 GHz	QAM-4	Hollow and solid core dielectric	15 m	8	–	[31]

In terms of integration and energy efficiency, the most promising interconnect technology seems to be based on planar spoof plasmons. If integration is not a primary design specification, but distance and interconnect flexibility, hollow dielectric waveguides outperform other interconnect technologies. The textured surfaces surveyed here should only be considered for scenarios such as airplane and drone fuselages, desktop chassis, etc., where existing metal parts can be textured to realize the interconnect without the need of additional elements. Thus, it is a useful approach to retrofit a communication channel. Given the large

disparity in terms of carrier frequency, bandwidth, and modulation scheme, we refrain from making any quantitative discussion.

5. Conclusion

The physical constraints of the dispersion and attenuation characteristics of geometrically induced terahertz surface wave interconnects on the energy efficiency of the links are investigated. It is shown that the capacity of such interconnects is primarily limited by the attenuation rather than dispersion. Therefore, the surface texture and roughness of terahertz surface wave interconnects will be key parameters for energy efficiency, and the choice of suitable surface texture and small roughness is an effective way to improve the energy efficiency of the links. This article pioneers a quantitative analysis of the data transmission capacity and energy efficiency of terahertz surface wave interconnects to highlight their limitations and provide a methodology for benchmarking.

Conflict of Interest

The authors declare no conflict of interest.

Data Availability Statement

The data that support the findings of this study are available from the corresponding author upon reasonable request.

[1] T. Kürner, D. M. Mittleman, T. Nagatsuma, *THz Communications Paving the Way Towards Wireless Tbps*, Springer, Cham **2022**.

[2] G. Xu, M. Skorobogatiy, *J. Infrared, Millimeter, Terahertz Waves* **2022**, *43*, 728.

[3] Z. Qi, X. Li, H. Zhu, *IET Microw. Antennas Propag.* **2018**, *12*, 254.

[4] A. Ishimaru, *Electromagnetic Wave Propagation, Radiation, and Scattering*, John Wiley & Sons, Inc., Hoboken, NJ **2017**.

[5] R. E. Collin, *Field Theory of Guided Waves*, Wiley-IEEE Press, New York, NY **1991**.

[6] S. A. Maier, *Plasmonics: Fundamentals and Applications*, Springer, New York, NY **2007**.

[7] C. H. Walter, *Traveling Wave Antennas*, Peninsula Publishing, Los Altos, CA **1991**.

[8] C. R. Williams, S. R. Andrews, S. A. Maier, A. I. Fernández-Domínguez, *Nat. Photonics* **2008**, *2*, 175.

[9] M. Navarro-Cía, M. Beruete, S. Agrafiotis, F. Falcone, M. Sorolla, S. A. Maier, *Opt. Express* **2009**, *17*, 18184.

[10] Y. Zhang, Y. Xu, C. Tian, Q. Xu, X. Zhang, Y. Li, X. Zhang, J. Han, W. Zhang, *Photonics Res.* **2018**, *6*, 18.

[11] E. Hendry, A. P. Hibbins, J. R. Sambles, *Phys. Rev. B* **2008**, *78*, 235426.

[12] M. G. Silveirinha, C. A. Fernandes, J. R. Costa, *IEEE Trans. Antennas Propag.* **2008**, *56*, 405.

[13] L. Shen, X. Chen, Y. Zhong, K. Agarwal, *Phys. Rev. B* **2008**, *77*, 075408.

[14] N. Dolatsha, C. Chen, A. Arbabian, *IEEE Trans. Terahertz Sci. Technol.* **2016**, *6*, 637.

[15] M. Naftaly, *Terahertz Metrology*, Artech House, Norwood, MA **2015**.

[16] S. Freer, J. Qing, P. Penchev, S. Dimov, S. M. Hanham, M. Navarro-Cía, *IEEE Trans. Terahertz Sci. Technol.*, under review.

[17] T. Kürner, ISG THz Activity Report **2022**, Valbonne - Sophia Antipolis.

[18] M. Navarro-Cía, J. E. Melzer, J. A. Harrington, O. Mitrofanov, *J. Infrared, Millimeter, Terahertz Waves* **2015**, *36*, 542.

[19] H. H. Nguyen, E. Shwedyk, *A First Course in Digital Communications*, Cambridge University Press, Cambridge, UK **2009**.

[20] ITU-R, Report ITU-R F.2416-0 **2017**, Geneva.

[21] E. Alon, M. Horowitz, *IEEE J. Solid-State Circuits* **2008**, *43*, 1795.

[22] M. Tytgat, N. V. Thienen, P. Reynaert, *Analog Integr. Circ. Sig. Process* **2015**, *83*, 55.

[23] Y. Liang, H. Yu, J. Zhao, W. Yang, Y. Wang, in *2015 IEEE/ACM Int. Symp. on Low Power Electronics and Design (ISLPED)*, Rome, Italy, July 22–24 **2015**, pp. 110–115.

[24] N. Van Thienen, W. Volkaerts, P. Reynaert, *IEEE J. Solid-State Circuits* **2016**, *51*, 1952.

[25] B. Yu, Y. Ye, X. L. Liu, Q. J. Gu, in *2016 IEEE Inter. Symp. or Radio-Frequency Integration Technology (RFIT)*, Taipei, Taiwan, August 24–26 **2016**, pp. 1–3.

[26] Y. Ye, B. Yu, X. Ding, X. Liu, Q. J. Gu, in *2017 IEEE MTT-S Int. Microwave Symp. (IMS)*, Honolulu, HI, June 4–9 **2017**, pp. 805–808.

[27] Y. Zhang, M. De Wit, P. Reynaert, in *2018 IEEE 44th European Solid State Circuits Conf. (ESSCIRC)*, Dresden, Germany, September 3–6 **2018**, pp. 234–237.

[28] S. R. Joy, M. Erementchouk, H. Yu, P. Mazumder, *IEEE Trans. Commun.* **2019**, *67*, 599.

[29] Y. Kim, B. Hu, R. Huang, A. Tang, C. Joye, T. Itoh, M.-C. F. Chang, *IEEE Trans. Terahertz Sci. Technol.* **2020**, *10*, 370.

[30] C.-Y. Liu, H.-E. Ding, S.-H. Wu, T.-L. Wu, *IEEE Trans. Microw. Theory Techn.* **2021**, *69*, 4010.

[31] A. Meyer, M. Schneider, in *2022 14th German Microwave Conf. (GeMiC)*, Ulm, Germany, May 16–18 **2022**, pp. 1–4.